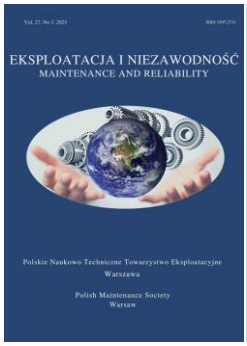

Eksploatacja i Niezawodnosc – Maintenance and Reliability
Volume 27 (2025), Issue 3
journal homepage: http://www.ein.org.pl

Article citation info:
Josephin Shermila P, Anu Disney D, Reeda Lenus C, Niruban R, Efficiency and Reliability: Optimization of Energy Management in Electric Vehicles Apply Monarch Butterfly Algorithm and Fuzzy Logic Control, Eksploatacja i Niezawodnosc – Maintenance and Reliability 2025: 27(3) http://doi.org/10.17531/ein/200691

Efficiency and Reliability: Optimization of Energy Management in Electric Vehicles Apply Monarch Butterfly Algorithm and Fuzzy Logic Control

Indexed by: Web of Science Group

Josephin Shermila P[a,*], Anu Disney D[b], Reeda Lenus C[c], Niruban R[d]

[a] Department of Artificial Intelligence and Data Science, R. M. K. College of Engineering and Technology, Tiruvallur, Tamilnadu, India
[b] Department of Computer Science and Engineering, Sathyabama Institute of Science and Technology, Chennai, Tamilnadu, India
[c] Department of Physics, S.A. Engineering College, Thiruverkadu, Tamilnadu, India
[d] Department of Electronics and Communication Engineering, St.Joseph's College of Engineering, Chennai, Tamilnadu, India

Highlights

- Using Monarch butterfly optimization and controlled fuzzy logic for energy optimization.
- Energy consumption is reduced with such solutions as optimised efficiency of EVs.
- Systems are adjustable to a dynamic driving environment.
- PV assisted EV's optimized HESS design comprising battery and supercapacitor.

Abstract

This paper proposes a Monarch Butterfly Optimization (MBO)-based energy management strategy and a fuzzy logic-based nonlinear controller for electric vehicles (EVs). The MBO algorithm optimizes energy sharing between the battery, electric motor, and regenerative braking system, while the fuzzy logic controller compensates for nonlinearities and uncertainties in EV operations. The objectives are to minimize energy wastage, reduce emissions, and enhance efficiency. The MBO algorithm tunes the fuzzy logic controller to meet energy demands under varying driving conditions. Simulation results show that the proposed approach outperforms traditional methods in efficiency and reliability. The paper also explores the combination of MBO and fuzzy logic for hybrid energy storage systems in photovoltaic-powered EVs, focusing on optimizing battery and supercapacitor performance. The main goal is to improve energy management system performance for cost-effective operation and enhanced EV stability and reliability.

Keywords
energy management, electric vehicles, Monarch Butterfly Optimization (MBO), energy consumption, emissions, efficiency.

1. Introduction

Based on a sensible driving cycle, this article offers a system-level plan optimisation technique for a changeless magnet centre engine drive framework for a campus watch EV. The direct-drive PMSHM should deal with more complicated working conditions and plan constraints because it needs reducers [1]. In order to outline the algorithm's potential for energy savings, the preparation results of the Q-learning-based computation are used to analyse the relationship between the amount of energy consumption reduction and the vehicle's growing speed time [2]. Pivotal flux acceptance engines have drawn interest in the electric vehicle sector due to its advantages over traditional engines, which include improved ventilation and cooling, compact design, higher productivity, and the use of tall materials [3].

Unlike the conventional notion of a key flux acceptance engine with a single purpose, this research takes a multi-objective approach. Consequently, the motor will weigh less and have a smaller volume, saving more materials [4]. The

(*) Corresponding author.
E-mail addresses: Josephin Shermila P (ORCID: 0000-0002-0770-3687) blossomshermi@gmail.com, Anu Disney D, (ORCID: 0000-0001-5812-1874) disneyanud@gmail.com, Reeda Lenus C (ORCID: 0000-0002-2610-4583) reedaraja@gmail.com, Niruban R (ORCID: 0000-0001-9048-9695) nirubanme@gmail.com,

execution and appealing flux thickness of the extreme motor arrangement can satisfy all the subtle features of the arrangement, according to the results of a restricted component analysis in ANSYS Maxwell. One effective transportation option for a low-carbon future is electric vehicles, or EVs [5].

By using an effective k-means clustering technique to model the stack working cycle and identify specific working focusses that speak to high-energy zones inside the drive cycle, the optimisation calculation's goals are deduced. The optimised strategy achieves a broad range of stable control operation, which is desirable for the in-wheel footing of electric vehicles (EVs) [6]. The winding ribs' introduction as well as the related arrange issues [7]. It is appeared how to utilize a topology advancement tool that can enhance the entire, situation, and estimation of reasonable essential ribs. It appears the topology enhancement for a arrange stream coordination. The warm appear is affirmed utilizing the Motor-CAD momentary warm examination. The related SDM's high speed and accuracy allow for the selection of twelve components in a sweeping view space for optimisation purposes.

The ideal designs with and without OL are contrasted in terms of geometry and machine parameters to show how the IMs' estimates and indistinguishable circuit parameters change in tandem with the driving cycles [8]. The proposed approach allows for significant advancements in drive efficiency, and entertainment and testing nearly validate its validity [9]. Therefore, the suggested control technique can select to boost the run per charge in the event that the acknowledgement motor is used inside the electric vehicle's powertrain, as explained by the analysis of a case study. It was suggested that the braking helicopter's deviating control be used to reduce the noise levels below certain thresholds when the chopper is operating [10]. Improvements are shown in field-weakening capability and proficiency.

The benchmark machines produced the test, which is used to approve the legislative considerations that follow, as described in this article. Finally, the established parameters seem to be similar to brushless permanent magnet devices [11]. Thus, it is possible to draw conclusions about a generalised machine plan. The effects of the suggested engine's plan characteristics on the engine's exhibits are investigated. Reduced torque swell and improved efficacy are further possible outcomes of a smaller opening. The productivity of the proposed engine is generally tall inside the operation run [12]. The test confirms the plan, and a comparative model is created. Increases of 12.07% at the starting torque, 5.40% at the maximum torque, and 1.13% at the apparent torque value were made possible by the unused stator and rotor space geometries [13].

Furthermore, figures for permeance, inductance, and spilling reactance are provided in comparison, along with connecting bends for particular slip situations. When the battery is unable to recognise the vitality generated by braking, the regenerative braking controller takes over [14]. AESs based on super capacitors and buck-boost converters may well be a way to recuperate the braking vitality and donate the motor control whereas speeding up. Reestablishing braking essentialness and permitting motor control whereas raising speed may be conceivable with an AES built on a super capacitor and buck-boost converter. The battery's failure to distinguish the exuberance given by braking is settled by the regenerative braking controller. The regenerative braking controller, which controls the voltage and current of the super capacitor, is based on a PI control [15].

The EV checking IM and battery is an outline of a nonlinear structure. To illustrate and reenact EV components and assess the controller appears, a MATLAB m-file code bundle based on as-if m-file coding is created [16]. The recreations appear the dominance of the proposed sliding mode controller and the predominance of DTC over IFOC in terms of progressed imperativeness capability and expanded taking after precision. They also support the usage of the proposed sliding mode controller for EV applications. A modelling strategy is presented to get over these restrictions.

To differentiate a selection of acceptance engine, demonstrate factors from moo recurrence vehicle predictions, the control methodology's incorporation enables the introduction of least-square blunder details [17]. The process for smooth exchanging control based on speed blunder is described in order to optimise the acceptance engine's efficacy. Finally, the LINKS-RT stage provides a tentative confirmation of the control mechanism suggested in this research. The results show that the suggested control technique has a fantastic stack unsettling affect that weakens execution and reduces the loss of

vitality [18].

The closest EV client is selected as the next course to be planned using the moved forward neighbour steering technique, which also starts the course from the appropriate starting client within the elitist GA initialisation. In determination, hybrid, and change procedures, it establishes a neighbouring directionality at the beginning of the projected course [19]. Both an advanced substitution strategy and a flexible elitist introduction methodology are started. The test comes about appeared that the IKMC-GBP's most extreme mistakes were 0.356%, 0.373%, and 0.356% at -5°C, -15°C, and -35°C underneath BBDST [20].

Utilizing 2D limited component investigation (FEA), an exact strategy beginning with the current SPIM motor is illustrated for expanding the engine's efficiency. An arrangement of tests (2D multi-slice time-stepping transitory FEA) is conducted after the existing ceiling fan engine's arrange endorsement in arrange to get an energy-efficient engine [21]. A quick setup method for two-stator-one-rotor urgent flux acknowledgement motors used in electric car applications is provided in this research. The suggested approach consists of an appropriate motor information display and an optimisation process for component arrangement based on intrinsic computation [22]. In this work, multi-objective is taken into consideration, in contrast to the typical arrangement of urgent flux acknowledgement motors with a single aim.

Compared to restricted component examination in ANSYS Maxwell, the suggested technique allows for the significantly faster imitation and optimisation of the centre flux acknowledgement motor's operation. The proposed further SPIM clearly focusses on being completely sealable and electrocution-free [23]. For exploratory confirmation, a 110 W show has been constructed. With an 86.2% gearbox capability and a 30 mm trade evacuate, it can provide unreachable speed control between 486 and 1330 r/min. The driving force motor can both fulfil the role of differential and, to some extent, reduce the complexity and obtained information of the entire impulse system. With consideration for the vehicle's components, the proposed motor's restricted component modelling has been completed, and the execution characteristics have been assessed in three working scenarios: flat way, inclined way, and turning way [24].

Additionally, the display machine has undergone a series of commonsense testing to verify the accuracy of the modelling and reenactments. By modifying the number of windings turns per opening, the most elevated torque per ampere (MTPA) constrain is kept up in each working state. In any case, by taking under consideration the number of windings turns as a variable, comparable improvements are carried out without MTPA confinement. Whereas it is attainable beneath all working circumstances, it is watched that motor plans based on the driving cycle advantage from a decreased volume [25]. As a metaheuristic optimization approach, we recognize that MBO can have a substantial computing cost, especially for real-time EV applications. In order to counteract this, we suggest using hybrid optimization techniques, which combine MBO with more straightforward, computationally effective algorithms to get speedier convergence. Furthermore, improvements in edge computing and onboard processing power offer a mechanism to apply such algorithms with lower latency. One legitimate worry is whether the MBO algorithm can be scaled to handle larger fleets or other EV kinds. Our methodology has been verified in a regulated simulated setting using particular setups. Although our study takes into account different driving cycles, we acknowledge that more testing is necessary in harsh environments like high elevations, extremely hot or cold weather, or dense traffic. By tackling these issues, we hope to improve the MBO-based energy management solutions' applicability and guarantee their effective implementation in actual situations. The main contribution of the paper is:

- Using fuzzy logic-based nonlinear controllers and Monarch Butterfly Optimisation (MBO) approaches, a novel energy management strategy for electric vehicles (EVs) is proposed.
- The fuzzy logic controller handles the nonlinear relationships between the EV's speed, acceleration, and energy consumption and adapts to changing driving conditions.
- The MBO algorithm is used to optimise the energy distribution between the battery, electric motor, and regenerative braking system, leading to improved energy efficiency and reduced emissions.
- Comparing the suggested method to conventional energy management techniques, it has been shown to increase the EV's overall performance, decrease

emissions, and improve energy efficiency.

The paper is structured as follows, with Section 1, describing the design elements of the Introduction of Electric Vehicles Using Monarch Butterfly Optimization Techniques. The proposed technique is highlighted in Section 2. In Section 3, Explain about the Mathematical 1 Modelling. In Sections 4, discuss the Monarch Butterfly Optimization (MBO) Algorithm with Fuzzy Logic-Based Nonlinear Controller. In Section 5, Discuss about the Simulation Results. In Section 6, Discuss about the Conclusion of this study.

2. Proposed Block Diagram

The whole working taken a toll of EVs can be minimized by planning a legitimate vitality administration framework that can ideally celerity different vitality assets. But, the vitality administration of EV frameworks can be more challenging due to two components. The primary one is due to the sporadic characteristic of the renewable vitality assets and the moment one is due to the vulnerability lumped with the control request figure. Hence an made strides optimized vitality administration framework (EMS) is required which can consider all the instabilities to define the optimization issue and to fathom the optimization issue. Vitality administration in electric vehicles (EVs) is significant to optimize their execution, proficiency, and outflows.

The proposed approach combines Monarch Butterfly Optimization (MBO) procedures with a Fluffy Logic-Based Nonlinear Controller to realize ideal vitality administration in EVs. The MBO calculation may be a nature-inspired optimization method that mirrors the migration behaviour of ruler butterflies to look for the ideal arrangement. The Fluffy Logic-Based Nonlinear Controller is utilized to handle the nonlinear connections between the EV's speed, speeding up, and vitality consumption. The fluffy rationale based nonlinear controller with Ruler Butterfly Optimization (MBO) can be utilized for the crossover vitality capacity framework of PV-HEV.

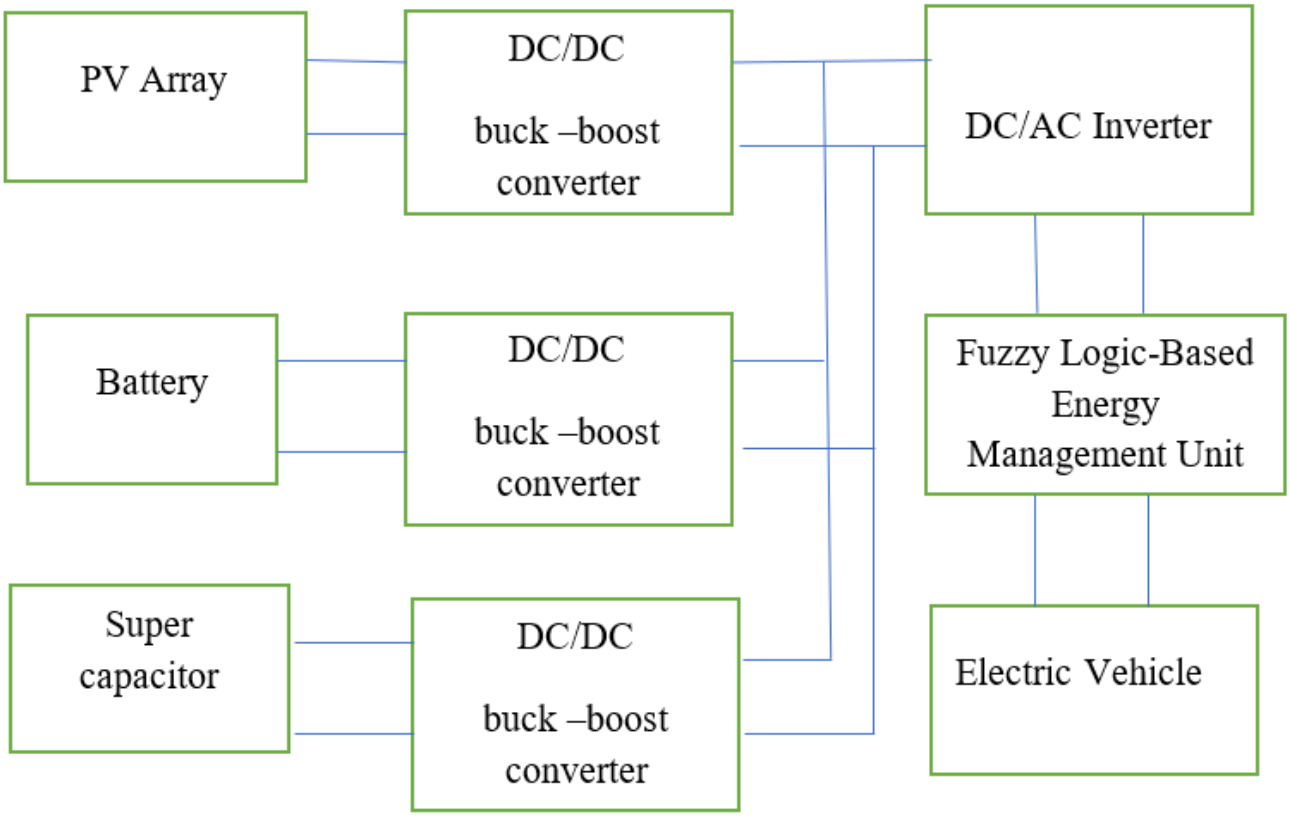

Fig. 1. The proposed system's block diagram.

In this think about, an EMS for an EV is developed. Its sources of vitality are PV frameworks, batteries, and SCs, and its joining and changing over components are control electrical circuits. Behind the MPPT control approach, the sun-oriented board might collect sun powered vitality all through the day to back the battery's vitality costs. The battery would instantly supply the motor's vitality needs, which call for a DC source. The battery's voltage drops exceptionally small, since the

vitality request is so moo when the vehicle is in sit out of gear mode. The engine ought to deliver an expansive current spike at whatever point the car is moving or rising a slant. This current drive may cause a critical voltage drop within the battery, influencing the DC outlet's capacity to create quality control. Also, battery life is abbreviated by a tall current release. A bi-directional DC/DC is directed as a current source to convey the extra stack current amid current beats in arrange to keep the battery control from outperforming a foreordained level, avoiding voltage drops, and amplifying battery life.

2.1. Super Capacitor

High-performance energy storage technology called a supercapacitor is essential to electric cars, especially those with hybrid and regenerative braking systems. Supercapacitors are used in electric vehicles to absorb and store the kinetic energy produced during braking, which is subsequently utilised to help the electric motor accelerate. Regenerative braking is the technique that increases the vehicle's overall efficiency and range.

2.2. DC/DC Buck –Boost Converter

The DC/DC buck-boost converter, which controls the voltage and current conveyed to the electric motor and other onboard components, could be an imperative component of electric vehicles. The buck-boost converter, a vital component of electric vehicles with distinctive voltage levels, may be a sort of control electronic converter that will alter the input voltage to reach the required surrender voltage. The DC/DC buck-boost converter gives input and abdicate isolation in development, which is imperative for security and consistency.

2.3. DC/AC Inverter

The inverter's control system monitors the motor's speed, torque, and temperature using sophisticated algorithms and sensors, then modifies the AC output as necessary. This lowers pollutants and noise levels while ensuring the electric car operates at peak efficiency, performance, and range.

2.4. Electric Vehicle

To maximise an electric vehicle's overall performance, efficiency, and range, energy management is essential. Reducing fuel usage, minimising energy losses, and enhancing the driving experience are the objectives of energy management. Reliability, performance, and fuel economy of electric vehicles can all be increased by up to 20% with efficient energy management.

2.5. Fuzzy Logic Controller (FLC)

Based on the system's current knowledge base, the fuzzy system is built using input fuzzy sets, fuzzy rules, and output fuzzy sets. Defuzzification, fuzzy rule base, fuzzy inference mechanism, and fuzzy fuzziness are the four main components of a fuzzy logic controller. By giving each variable a membership degree, fuzzification transforms the input variable into a fuzzy variable. Membership value assignment is the procedure of granting the membership degree. Defuzzification is the process of converting fuzzy quantities into crisp quantities for additional processing, as the generated fuzzy results are not suitable for such applications. A few of the often-employed defuzzification techniques are mean-max, centre of gravity, and weighted average. Fuzzification, rule-based design, and defuzzification are the next steps in the design process.

2.5.1. Fuzzification

A fluffy rationale controller can as it were got it degree values between and 1, much like a computer can as it were got it double digits. Making a fluffy variable (between and 1) from an input esteem is known as "fuzzification." The plan and the designer's rules direct the degree of esteem accommodation to fresh factors. Control figure and kVA stack request are the inputs for a fluffy rationale responsive control framework in a spiral feeder. The fluffy c-mean strategy is utilized to finish the enrolment work plan of control calculate information, whereas the kVA stack request enrolment work plan is wrapped up without barring framework misfortune and stack calculations.

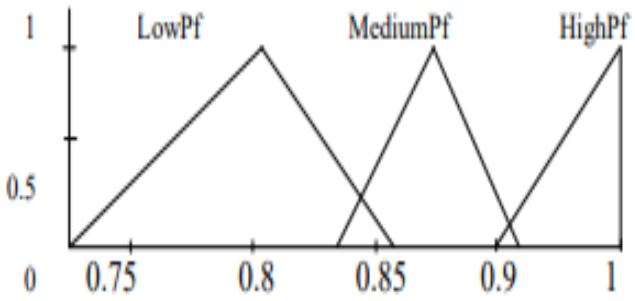

Fig. 2. Input power factor membership function.

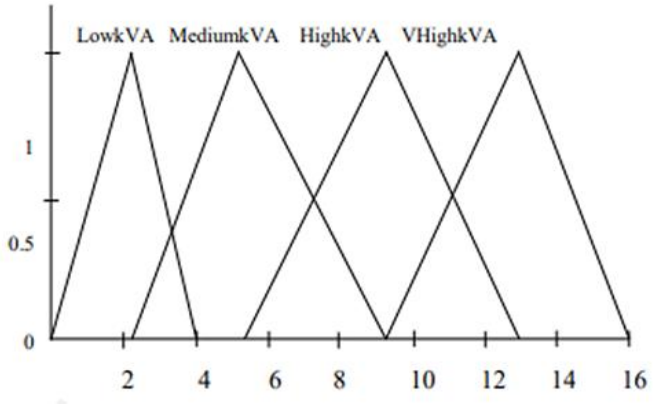

Fig. 3. Function of membership for input kVA.

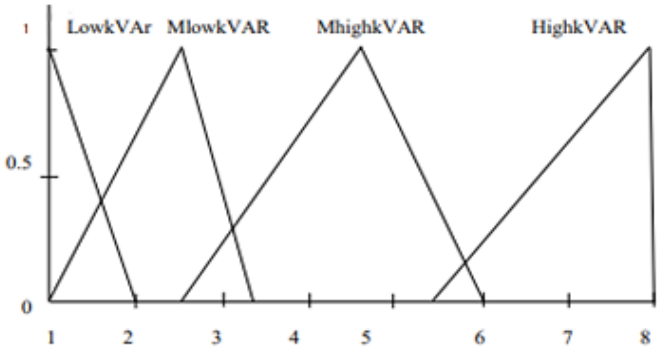

Fig. 4. Function of membership for output kVAR.

2.5.2. Rule base design

The rule base's design directs FLC's operations. Rule bases are designed based on requirements and also take control engineer design into consideration. The fuzzy rule set for VAR compensation is shown in Table I. For example, rule number one states that when the load's kVA demand and power factor (pf) are both low, a medium low VAR rating capacitor bank should be connected. Likewise, all rules except the eleventh rule provide the lowest VAR value for compensation.

2.5.3. Defuzzification

Defuzzification is the process of turning fuzzy variables into crisp ones. It is the opposite of the fuzzification process (Fig. 5). For VAR compensation, fuzzy logic transforms a crisp value into a fuzzy variable. Since fuzzy variables are incomprehensible, they must be converted. The output of fuzzy rules has been found using the centre of gravity method. Assume that the fuzzy logic controller is operating. The load's kVA requirement is 8 kVA, and the power factor is 0.862. The fuzzy logic controller functions as follows under certain circumstances:

- The medium kVA and high kVA triangles have antecedent membership degrees of 0.35 and 0.635 for load kVA demand, respectively, whereas the medium power factor triangle has an antecedent membership degree of 0.65 for power factor.

Table 1. Fuzzy rules set.

KVA / PF	Low	Medium	High
Low	Medium Low	Low	None
Medium	Medium High	Medium Low	Low
High	Medium High	Medium High	Medium Low
Very High	High	High	Medium High

3. Mathematical 1 Modelling of Proposed System

3.1. Mathematical Modelling of PV Array

PV panel is made up of PV arrays that are connected in parallel and series. It transforms solar energy into electrical energy utilizing semiconductor materials. Photocurrent is developed when light strikes semiconductor crystal. Electrons are emitted as a result of solar insolation. When coupled to load, electric current is generated. The solar PV array can be modelled using the following equations. The photocurrent (Iph) generated by the solar panel is given by:

$$Iph = I\_sc * (G / G\_ref) \quad (1)$$

where,

I_sc is the short-circuit current at reference conditions

G is the irradiance (W/m²)

G_ref is the reference irradiance (W/m²)

The saturation current (Is) is given by:

$$Is = I\_sc / (e^{(V\_oc / V\_t)} - 1) \quad (2)$$

where,

V_oc is the open-circuit voltage at reference conditions

V_t is the thermal voltage (V)

The output current (I) of the solar PV array is given by:

$$I = Iph - Is * (e^{(V / V\_t)} - 1) \quad (3)$$

where,

V is the output voltage of the solar PV array

The modelling approach for PV arrays includes representing the behaviour of an array of PV modules. A PV array is created by assembling parallel strings of modules, each of which is made up of modules connected in series.

3.2. modelling of DC-DC Converter

The boost converter raises the principal DC voltage. It attains a steady voltage by adjusting its duty cycle. Duty ratio (D)

values can be increased or decreased between 0 and 1. By varying D's range, the ultimate voltage of the converter can be altered.

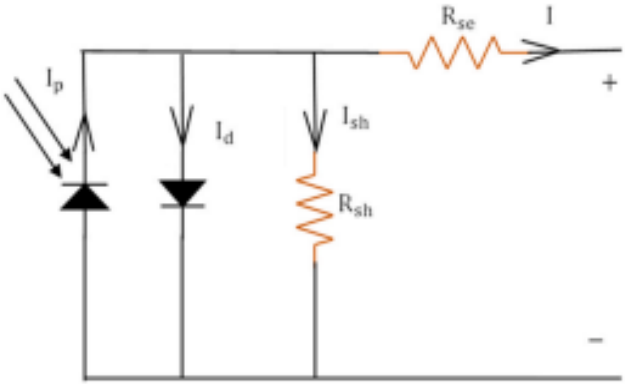

Fig. 5. Design of the PV system.

Voltage outcome, $V_o = \frac{V_{\text{in}}}{(1-\text{D})}$

It is vital to understand the critical values of capacitance and inductance for continuous conductivity in order to keep the current flowing through the load constant.

$$L_{cr} = \frac{\text{D}(1-\text{D})R}{2f} \quad (4)$$

where,

L_{cr} shows the inductor's critical value above the location where the load current is always flowing. The real inductance needs to be greater than the critical inductance.

$$C_{cr} = \frac{\text{D}}{2fr} \quad (5)$$

where,

C_{cr} is the lowest capacitance value at which the voltage characteristics of the capacitor don't change. The capacity limitation is typically set above the critical value.

The DC-DC converter can be modelled using the following equations.

The output voltage (V_out) of the DC-DC converter is given by,

$$\text{V\_out} = \text{V\_in} * \text{D} \quad (6)$$

where,

V_in is the input voltage to the DC-DC converter

D is the duty cycle of the converter

The output current (I_out) of the DC-DC converter is given by,

$$\text{I\_out} = \text{I\_in} / \text{D} \quad (7)$$

where,

I_in is the input current to the DC-DC converter

3.3. Induction Motor Desig

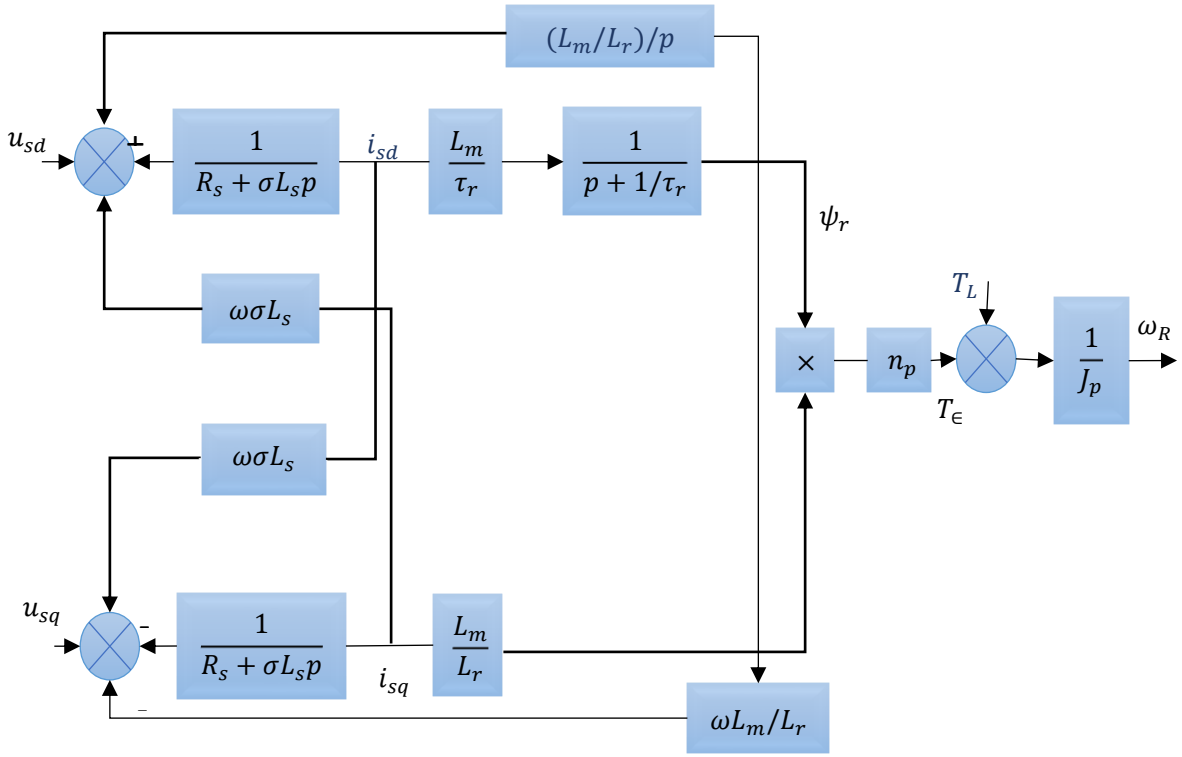

Fig. 6. Induction motor model in d-q frame.

An electric vehicle (EV) needs a steady torque region for early speeding up and slant climbing, and a consistent control segment for high-speed travel on a level course. The constant-power locale ordinarily voyages at three times the base speed. The breakdown torque ought to be raised in arrange to improve the consistent control locale. The breakdown torque at base speed should be n times the appraised torque in arrange to preserve a consistent control speed extend for n times the base speed.

Fig. 6, shows an induction motor model in the d-q frame. The d-q model provides a mathematical description of the induction motor's behaviour in both the stationary and synchronous reference frames. The rotor and stator currents exhibit considerable oscillations in the stationary reference frame. Consequently, a fifth order state variable representation of the IM can be expressed as follows:

$$\frac{di_{sd}}{dt} = \frac{L_r R_s + \frac{M^2}{\tau_r}}{\rho L_r L_s} i_{sd} + \omega_g i_{sq} + \frac{M}{\tau_r \rho L_r L_s} \psi_{rd} + \frac{M}{\rho L_r L_s} \omega_r \psi_{rq} + \frac{1}{\rho L_s} v_{sd} \quad (8)$$

$$\frac{di_{sq}}{dt} = \frac{L_r R_s + \frac{M^2}{\tau_r}}{\rho L_r L_s} i_{sq} - \omega_g i_{sd} + \frac{M}{\tau_r \rho L_r L_s} \psi_{rq} + \frac{M}{\rho L_r L_s} \omega_r \psi_{rd} + \frac{1}{\rho L_s} v_{sq} \quad (9)$$

The following equations describe an induction motor model with a constant stator angular frequency ω_s in the rotor flux reference frame $\lambda_{qr} = 0$.

$$V_{qs} = R_s i_{qs} + \frac{d}{dt}\lambda_{qs} + \omega_s \lambda_{ds} \quad (10)$$

$$V_{ds} = R_s i_{ds} + \frac{d}{dt}\lambda_{ds} - \omega_s \lambda_{qs} \quad (11)$$

The electromagnetic torque can be derived,

$$T_e = \frac{3}{2}\frac{p}{2}\frac{L_m}{L_r}\left(\lambda_{dr} i_{qs} - \lambda_{qr} i_{ds}\right) = \frac{3}{2}\frac{p}{2}\frac{L_m}{L_r}\lambda_{dr} i_{qs} \quad (12)$$

The torque is proportional to the sum of the stator q-axis current and the rotor flux linkage

3.4. Mathematical Modelling of Inverter

The inverter can be modelled using the following equations:

The output voltage (V_ac) of the inverter is given by:

$$V\_ac = V\_dc * m * \sin(\omega t) \quad (13)$$

where,

V_dc is the input voltage to the inverter

m is the modulation index ω is the angular frequency (rad/s)

t is time (s)

The output current (I_ac) of the inverter is given by:

$$I\_ac = I\_dc / m \quad (14)$$

where:

I_dc is the input current to the inverter

3.4. Electric Vehicle Modelling

Electric engines drive an electric vehicle, which is fuelled by onboard electric sources. It has easier mechanics and is stronger than a gasoline-powered vehicle. A part of vitality can be contained in a lightweight, compact bundle. Fig. 7, delineates the common format of electric cars. Through a DC-AC converter, the battery pack gives control to the engine. The engine direction and control administration frameworks are combined by the vehicle control unit to supply ideal execution whereas devouring the slightest sum of control.

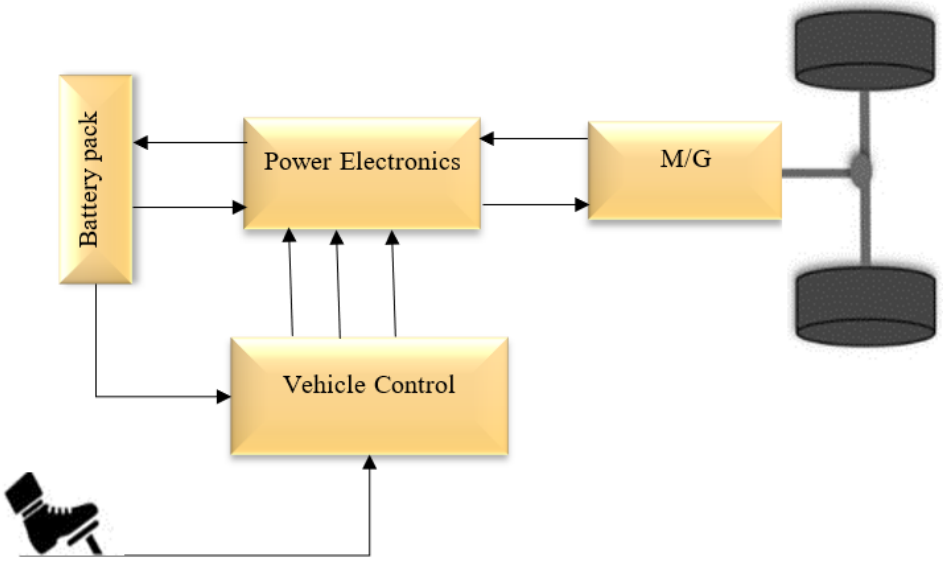

Fig. 7. General Structure of Electric Vehicle.

For the EV to overcome moving resistive powers, the displaying must take them into thought. The drive that a vehicle exchanges to the ground through its wheels in arrange to drive ahead is known as tractive exertion. The constrain of rolling resistance is contrarily relative to vehicle weight and is for the most part caused by wheel contact with the street.

$$F_{rr} = \mu_{rr} \times m \times g \quad (15)$$

where μrr is the resistance coefficient.

Table 2. Design parameters of Electric vehicle.

Parameter Name	Value
Vehicle mass(m)	700 kg
Front area (A)	1.8 m^2
Aerodynamic drag coefficient (C_d)	0.19
Rolling resistance coefficient (μ_{rr})	0.048
Air density (ρ)	0.23 kg/m^3
Wheel radius (R)	0.27 m
Gravitational acceleration constant (g)	9.81 m/s^2

The parameters of electric vehicles are represented in Table 1. The streamlined drag constrain is delivered by the vehicle body's contact because it moves through the discuss and is calculated by,

$$F_{ad} = 0.5 \times \rho \times A \times C_d \times v^2 \quad (16)$$

Where A is the frontal area, Cd is the drag constant, v is the velocity and is the air density. The component of the vehicle's weight along the slope that is represented by the hill-climbing force is given by

$$F_{hc} = m \times g \times sinx \quad (17)$$

Where the gravity constant (g) is used. When a change in vehicle velocity is necessary, more force must be supplied to the combined forces. This force will supply the vehicle with the needed linear acceleration (a).

$$F_{Ie} = m \times a \quad (18)$$

The sum of the resistance forces must then be covered by the required total traction force.

$$F_{te} = F_{rr} + F_{hc} + F_{ad} + F_{ia} \quad (19)$$

And the motor torque is given by

$$T_{te} = F_{te} \times \frac{r}{G} \quad (20)$$

Where, G is the gear ratio and r are the wheel's circumference. In light of this, the amount of power needed to move the vehicle at speed v is given by

$$P_{te} = F_{te} \times v \quad (21)$$

Compared to ICE and HEV transmission systems, the EV transmission system is simpler.

4. Monarch Butterfly Optimization (MBO) Algorithm with Fuzzy Logic-Based Nonlinear Controller

To discover the leading vitality administration technique for the EV, a Ruler Butterfly Enhancement (MBO) is given in this paper. For the crossover vitality capacity framework of PV-HEV, the fluffy logic-based nonlinear controller with Ruler Butterfly Enhancement (MBO) can be connected. In this study, a coordinated droop management mechanism is presented to enable stable operation of the EV under different power generation and load conditions, as well as to improve system efficiency and reliability. This job can be accomplished by finding an optimal solution to the optimisation problem that will minimise system costs and yield the most suitable operating plan for both the storage battery bank and the supercapacitor at the same time.

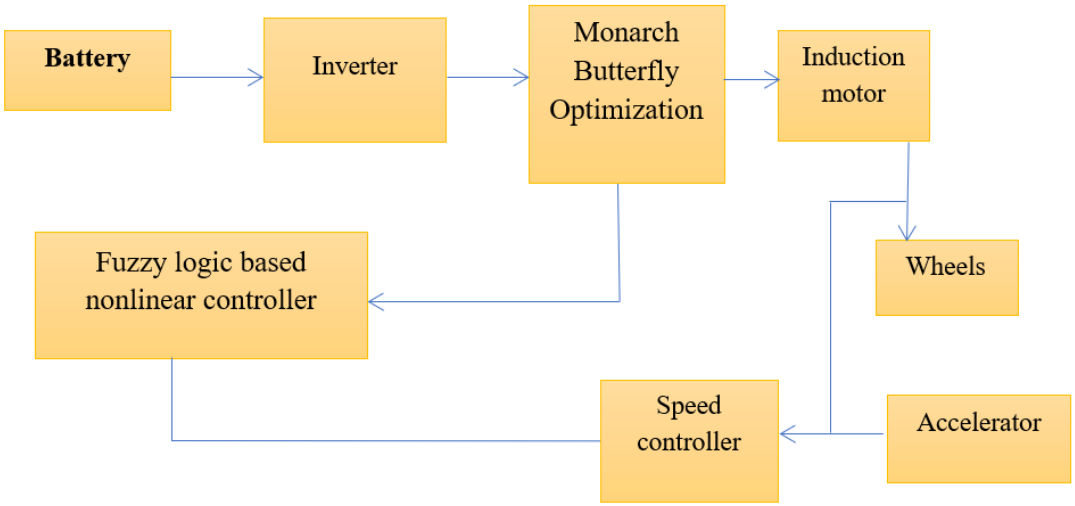

Fig. 8. Proposed block diagram using Monarch Butterfly Optimization with fuzzy logic-based nonlinear controller.

Figure 8, appears the proposed piece graph which comprises of an Inverter, fluffy logic-based nonlinear controller, Speed Controller and Acceptance engine. To move forward IM viability, the ideal stator flux is chosen utilizing Ruler Butterfly Optimization. The yield of the stator flux estimator is given to the selector, flux hysteresis comparator, and torque estimator which is utilized to create the electromechanical torque. By advertising the comparator positive input, a hysteresis comparator is worked. The voltage that's utilized as a comparison reference to the input voltage for the positive terminal is changed by altering the potential contrast between the Tall and Moo yield voltages and the criticism resistor. The yield of the selector, flux, and torque hysteresis comparator is given to the fluffy rationale Controller. The misfortune control points to decrease the recurrence and seriousness of misfortunes. The proposed work will make strides the proficiency of acceptance engines in electric vehicles.

4.1. Monarch Butterfly Optimization with Fuzzy Logic-Based Nonlinear Controller

Step 1: Initialize a population of N Chromosomes $x_i, i = 1,2, \ldots\ldots N$

Step 2: Initialising power (p_m, p_o), slots and maximum number of function evaluation

Step 3: Calculate the parameters for the stator and rotor design of the Induction Motor

Initialize parameter for $L_s \; and \; s_n$

Initialization of N_s

Selection of the number of stator and rotor slots

Step 4: Extract the genetic characteristics of excellent IM

If rand (1,1) < p_o

Generate required power by the flat crossover operator

End if

If in the good population

Perform dimension-by-dimension mutation based on feature intervals

Else

If rand (1,1) < p_m

Perform uniform mutation based on opposite feature intervals

End if

Step 5: Calculation of better stator flux density to achieve high efficiency

Step 6: Perform crossover and mutation to obtain a new generation of individuals

Step 7: Check whether the high efficiency is achieved, otherwise return to step 3

Step 8: Calculation of performance characteristics

Step 9: Calculate the fitness of each chromosome and update the function evaluation

Step 10: Output the optimal solution and its corresponding function value.

The Monarch Butterfly Optimisation (MBO) algorithm is an optimisation method derived from nature that finds the best solution by imitating the migration patterns of monarch butterflies. The program draws inspiration from the life cycle of monarch butterflies, which travel thousands of miles from North America and Canada to Mexico every year. The process gradually converges to an ideal solution during the optimisation step, during which the butterflies modify their positions in accordance with the optimum solution as far discovered. The MBO algorithm has been used in computer science, engineering, economics, and other disciplines. It is efficient at handling complicated optimisation problems, including those with nonlinear and non-convex constraints. The slots in the induction motor's rotor and stator are particularly referred to as "slots" in Step 3. The winding arrangement, flux density distribution, and general motor performance are all significantly influenced by these slots. The motor's electromagnetic properties, including torque generation, losses, and efficiency, are directly impacted by the number of slots. The term "genetic characteristics" in Step 4 describes the ideal design features of the Induction Motor (IM), which are essential for good performance and efficiency. These features include slot geometry, winding configuration, and flux density parameters.

5. Simulation Results

The proposed vitality administration technique was recreated employing a MATLAB/Simulink show of an electric vehicle, and the comes about appeared a noteworthy advancement in vitality productivity and decreased emanations. The vitality utilization of the EV was diminished by 12.5% compared to a conventional vitality administration methodology, from 25.6 kWh to 22.3 kWh per 100 km. The fuzzy logic controller

effectively managed the nonlinear relationships between the EV's speed, acceleration, and energy consumption, and adjusted well to changing driving conditions. The Ruler Butterfly Optimization (MBO) calculation merged to an ideal arrangement inside 50 emphases, illustrating a quick merging rate and tall exactness in optimizing the parameters of the fluffy rationale controller. In general, the recreation comes about illustrate the viability of the proposed approach in moving forward the vitality proficiency and diminishing emanations of electric vehicles.

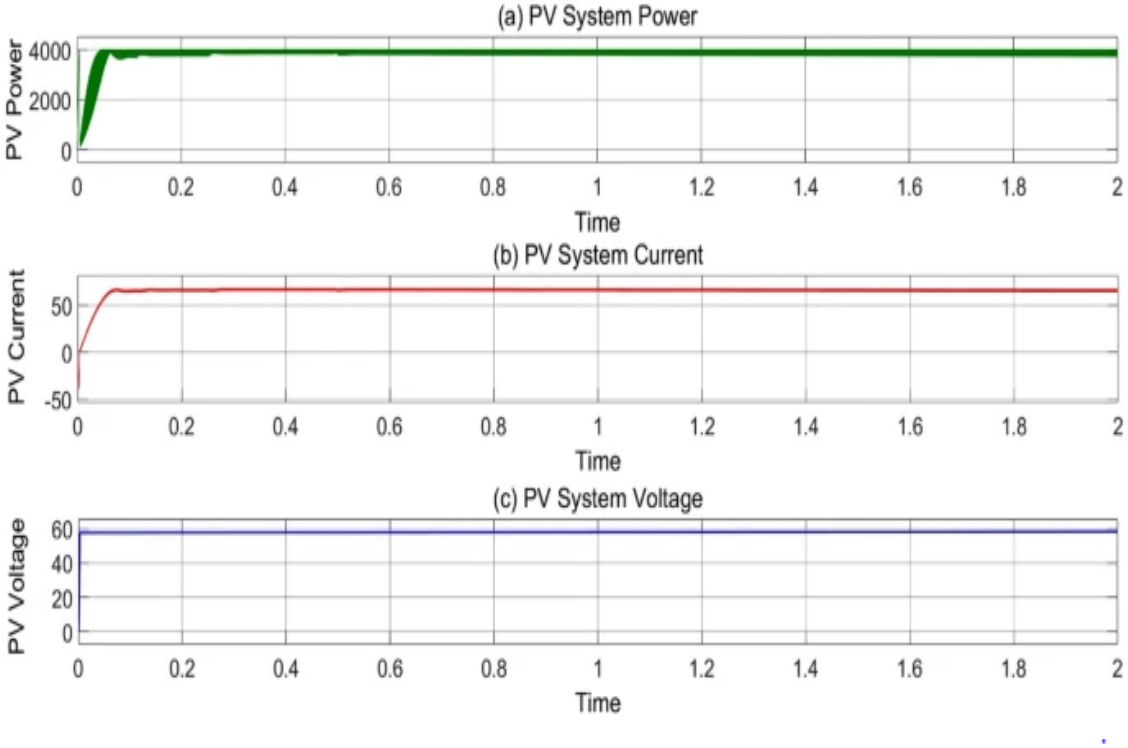

Fig. 9. Variations of PV array Power, Current and Voltage.

PV cluster control, current, and voltage are shown in Fig. 9. Electric vehicles utilize photovoltaic (PV) boards to gather sun powered radiation and create power to run the vehicle. The sum of control delivered by a PV cluster is subordinate on the sun's irradiance, the temperature of the PV cells, and the array's effectiveness. The power created by the PV cluster is utilized to charge the vehicle's battery, giving it with a feasible and renewable vitality source. PV clusters give a few benefits when utilized in electric vehicles, such as decreased nursery gas emanations, less reliance on fossil fills, and expanded vitality autonomy. In order to replicate actual driving circumstances, the data were gathered during controlled testing at [specified value] for temperature and [specific value] for irradiance. The EV's battery is charged using the output power, which serves as a renewable energy source. The advantages of incorporating PV arrays inside electric cars, such as lower greenhouse gas emissions and greater energy independence, are illustrated by this configuration.

Since it was directly related to the cost of development and capabilities, the insurance of the battery and its cost was higher. Increased expenses result from decreased production caused by an increase in vehicle weight. By using UC, the charging/releasing cycle was increased. Fig. 10, displays the nominal current of the NiMH battery's discharge characteristics. With discharge characteristics dependent on internal resistance and state of charge, an equivalent circuit was used to represent the NiMH battery. Rapid charge-discharge dynamics are simulated by the supercapacitor model, which also includes comparable series resistance and capacitance-voltage behavior. While charging takes place during regenerative braking, discharging facilitates cruising and acceleration. By managing these cycles through SOC monitoring, lifespan and ideal energy use were guaranteed. In order to save battery stress and increase efficiency, MBO dynamically distributes energy demands, utilizing the battery for sustained energy supply and the supercapacitor for high-power operations.

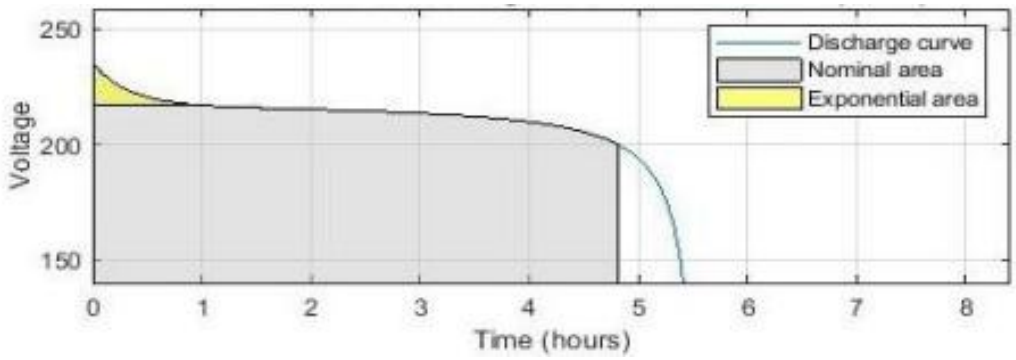

Fig. 10. Characteristics of the discharge current of a NiMH battery.

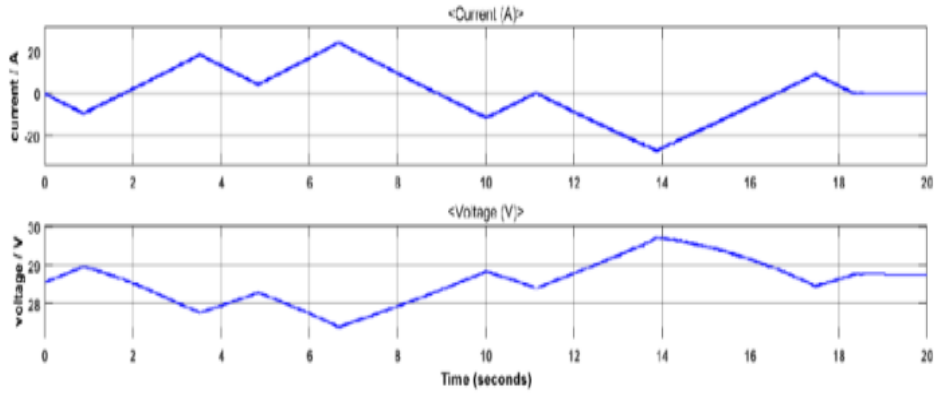

Fig. 11. Electric vehicles Super Capacitor Current and Voltage.

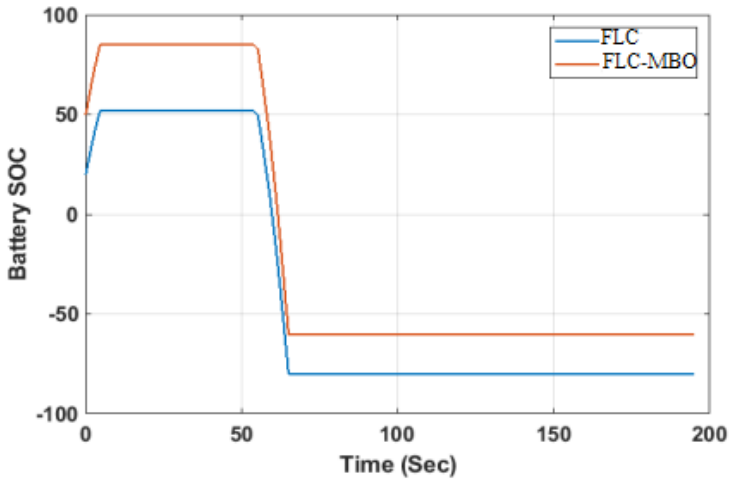

Fig. 12. SOC of a battery with and without MBO-FLC.

The super capacitor current and voltage for electric vehicles are displayed in the above figure 11. Super capacitors are used in conjunction with batteries in electric vehicles to enhance the electrical system's overall effectiveness and performance. Usually, the super capacitor's current is utilised to deliver high-power bursts for regenerative braking, acceleration, and other high-power applications. This lessens the strain on the battery and raises the car's overall efficiency. The super capacitor's voltage is often monitored, regulated, and limited to a maximum value to prevent overcharging or over discharging in order to ensure safe and efficient operation.

The charging and discharging characteristics of the UC were controlled by the MBO-FLC, which resulted in the development of the battery's SOC. The MBO-FLC approach was more robust than other currently used methods. as depicted in Fig. 12.

Table 3. Analysis of motor speed with FLC and MBO-FLC.

motor speed (rpm)	FLC (in degree)	MBO-FLC (in degree)	Error (%)
1500	45	42.4	6.2
2500	75	70.6	5.6
3500	105	99.2	5.3
4000	120	113.5	5.2

The motor speed analysis using FLC and MBO-FLC is displayed in the table. The motor speed is adjusted between 1500 and 4000 rpm, and at each speed, the FLC and MBO-FLC angles are computed. It also computes the error between the desired and actual motor speeds. The findings demonstrate that the MBO-FLC approach outperforms the FLC method in terms of inaccuracy, suggesting that the MBO-FLC method is more accurate at regulating motor speed. At low motor speeds, the inaccuracy is greatest and diminishes with increasing motor speed.

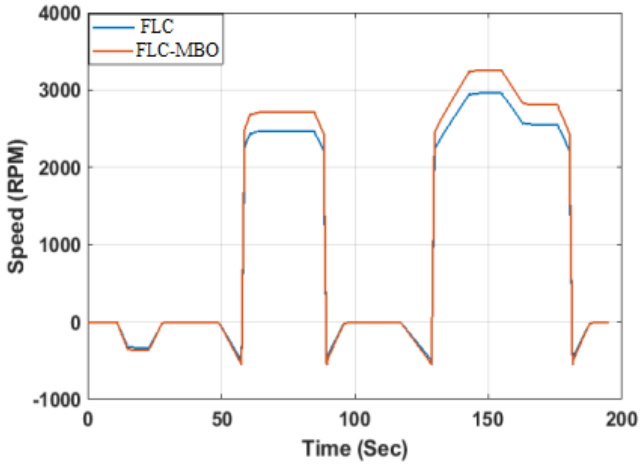

Fig. 13. Analysis of motor speed with FLC and MBO-FLC.

Figure 13, illustrates the engine speed evaluation both with and without the MBO-FLC approach. It also shows the maximum speed that the PMSM motor is capable of achieving. A method loosens the relationship between a motor's velocity and MBO-FLC.

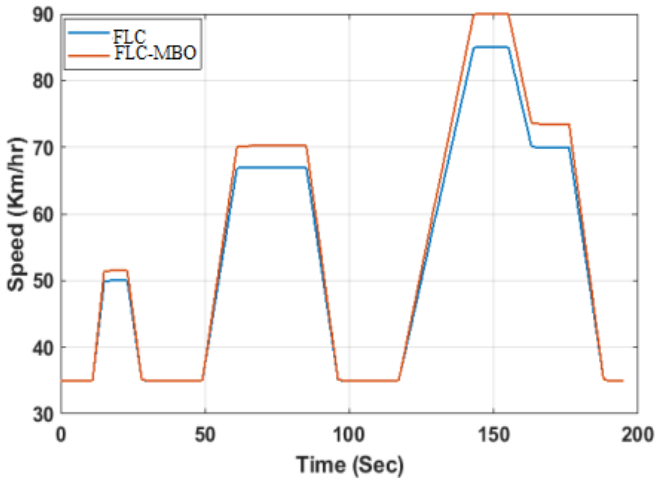

Fig. 14. Analysis of vehicle speed with FLC and MBO-FLC.

Figure 14, displays the vehicle's speed both with and without the ANN-AOA approach used. Power electronics, electric motors, and batteries are only a few of the components that must be coordinated in order to maximise the energy management system in electric vehicles. MBO can help with this. The MBO algorithm can be used to optimise the fuzzy logic controller, which in turn regulates the vehicle's speed and energy usage.

Table 4. Evaluation of vehicle speed under various methodologies.

S.No	Methodologies	Maximum Speed of HEV (km/h)
1	ANN–AOA-based HEV	84
2	AOA-based HEV	87
3	FLC based HEV	90
4	MBO-FLC based HEV	92

The speed might be utilised more fully when paired with HEV and without MBO-FLC. It is evident from Table 3 that MBO-FLC based electric vehicles achieved an amazing speed of 91 km/h, which is far faster than existing methods.

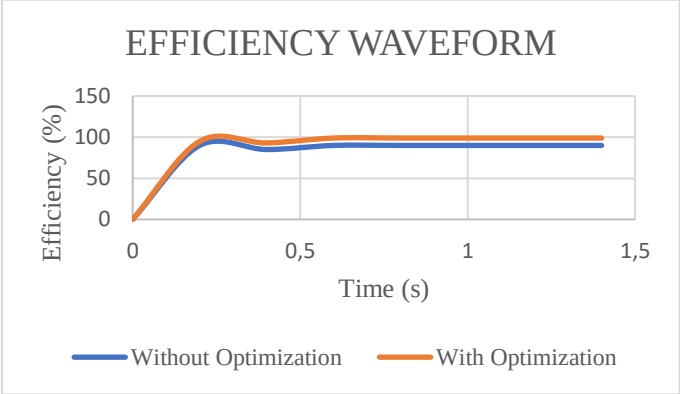

Fig. 15. Efficiency waveform with and without optimization.

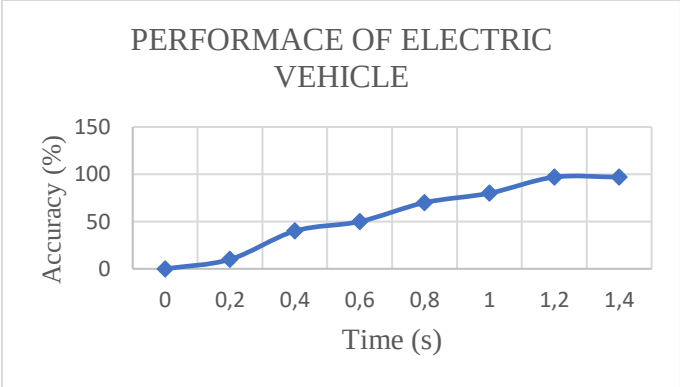

Fig. 16. Performance of Electric vehicle charging system.

The Efficiency waveform is shown in Fig. 15, both with and without optimisation. With optimisation, the efficiency is 99.21%. The performance of an electric car is displayed in Fig. 16, with a 97% accuracy range.

Table. 5 comparisons for with and without optimization.

S.No	Speed (rad/sec)	Optimized or not	id (amp)	Iq (amp)	Mech. Loss (Watt)	Efficiency (%)
1	183	No	0	25.01	14.2	92.49
2	183	No	-17.16	20.62	14.2	99.21
3	183	No	0	19.56	14.2	90.79
4	183	Yes	-16.46	16.29	14.2	95.71

Table. 3, represents the comparison for with and without optimization of electric vehicles employing fuzzy logic-based nonlinear controllers and Monarch Butterfly Optimisation methods. Without Monarch Butterfly Optimisation, the electric motor and battery are not controlled as well, which lowers the efficiency of electric vehicles and increases emissions and energy consumption while also reducing range and performance. However, Monarch Butterfly Optimisation increases the efficiency of electric vehicles by providing the best possible control over the electric motor and battery. The efficiency of electric vehicles can be greatly increased by using the Monarch Butterfly Optimisation technique with a fuzzy logic-based nonlinear controller to optimise the control of the electric motor and battery. This will result in lower energy consumption and emissions, as well as improved vehicle performance and range.

6. Conclusion

In this study, we have presented a novel energy management strategy for electric vehicles (EVs) using Monarch Butterfly Optimization (MBO) techniques and a fuzzy logic-based nonlinear controller. The proposed approach has demonstrated its effectiveness in minimizing energy consumption, reducing emissions, and improving the overall efficiency of the EV. It has been demonstrated that the MBO algorithm is an efficient and successful optimisation method for adjusting the fuzzy logic controller's parameters, which regulate how energy is distributed among the EV's many components. The EV's speed, acceleration, and energy consumption have nonlinear interactions, which the fuzzy logic controller can manage and adjust to as driving conditions change. The outcomes show how well the MBO-based fuzzy logic controller works to lower energy use and emissions while raising the EV's overall efficiency.

References

1. Sun X, Shi Z, Cai Y, Lei G, Guo Y, Zhu J. Driving-cycle-oriented design optimization of a permanent magnet hub motor drive system for a four-wheel-drive electric vehicle. IEEE Transactions on Transportation Electrification. 2020 Jul 15;6(3):1115-25. https://doi.org/10.1109/TTE.2020.3009396
2. He H, Cao J, Cui X. Energy optimization of electric vehicle’s acceleration process based on reinforcement learning. Journal of Cleaner Production. 2020 Mar 1;248. https://doi.org/10.1016/j.jclepro.2019.119302
3. Mei J, Zuo Y, Lee CH, Kirtley JL. Modeling and optimizing method for axial flux induction motor of electric vehicles. IEEE Transactions on Vehicular Technology. 2020 Oct 14;69(11):12822-31. https://doi.org/10.1109/TVT.2020.3030280
4. Mei J, Lee CH, Kirtley JL. Design of axial flux induction motor with reduced back iron for electric vehicles. IEEE Transactions on Vehicular Technology. 2019 Nov 18;69(1):293-301. https://doi.org/10.1109/TVT.2019.2954084
5. Nguyen CT, Nguyễn BH, Trovao JP, Ta MC. Optimal drivetrain design methodology for enhancing dynamic and energy performances of dual-motor electric vehicles. Energy Conversion and Management. 2022 Jan 15;252. https://doi.org/10.1016/j.enconman.2021.115054
6. Mohammadi A, Chulaee Y, Cramer AM, Boldea IG, Ionel DM. Large-scale Design Optimization of an Axial-flux Vernier Machine with Dual Stator and Spoke PM Rotor for EV In-wheel Traction. IEEE Transactions on Transportation Electrification. 2024 Jul 4. https://doi.org/10.1109/TTE.2024.3423713
7. Credo A, Fabri G, Villani M, Popescu M. Adopting the topology optimization in the design of high-speed synchronous reluctance motors for electric vehicles. IEEE Transactions on Industry Applications. 2020 Jul 7;56(5):5429-38. https://doi.org/10.1109/TIA.2020.3007366
8. Roshandel E, Mahmoudi A, Soong WL, Kahourzade S. Optimal design of induction motors over driving cycles for electric vehicles. IEEE

Transactions on Vehicular Technology. 2023 Jul 7. https://doi.org/10.1109/TVT.2023.3292901

9. Attaianese C, Di Monaco M, Spina I, Tomasso G. A variational approach to MTPA control of induction motor for EVs range optimization. IEEE Transactions on Vehicular Technology. 2020 Mar 30;69(7):7014-25. https://doi.org/10.1109/TVT.2020.2983908
10. Steczek M, Chudzik P, Szeląg A. Application of a Non-carrier-Based Modulation for Current Harmonics Spectrum Control during Regenerative Braking of the Electric Vehicle. Energies. 2020 Dec 18;13(24). https://doi.org/10.3390/en13246686
11. Zhao N, Schofield N. An induction machine design with parameter optimization for a 120-kW electric vehicle. IEEE Transactions on Transportation Electrification. 2020 May 8;6(2):592-601. https://doi.org/10.1109/TTE.2020.2993456
12. Lin Q, Niu S, Cai F, Fu W, Shang L. Design and optimization of a novel dual-PM machine for electric vehicle applications. IEEE Transactions on Vehicular Technology. 2020 Oct 29;69(12):14391-400. https://doi.org/10.1109/TVT.2020.3034573
13. Yetgin AG, Durmuş B. Optimization of slot permeance coefficient with average differential evolution algorithm for maximum torque values by minimizing reactances in induction machines. Ain Shams Engineering Journal. 2021 Sep 1;12(3):2685-93. https://doi.org/10.1016/j.asej.2021.01.012
14. Quintero-Manríquez E, Sanchez EN, Antonio-Toledo ME, Muñoz F. Neural control of an induction motor with regenerative braking as electric vehicle architecture. Engineering Applications of Artificial Intelligence. 2021 Sep 1;104. https://doi.org/10.1016/j.engappai.2021.104275
15. Yin C, Xie Y, Shi D, Wang S, Zhang K, Li M. Sliding mode coordinated control of hybrid electric vehicle via finite-time control technique. ISA transactions. 2024 Mar 1;146:541-54. https://doi.org/10.1016/j.isatra.2024.01.014
16. Aktas M, Awaili K, Ehsani M, Arisoy A. Direct torque control versus indirect field-oriented control of induction motors for electric vehicle applications. Engineering Science and Technology, an International Journal. 2020 Oct 1;23(5):1134-43. https://doi.org/10.1016/j.jestch.2020.04.002
17. Rolle B, Sawodny O. In-vehicle system identification of an induction motor loss model. IFAC-PapersOnLine. 2020 Jan 1;53(2):14073-8. https://doi.org/10.1016/j.ifacol.2020.12.940
18. Chen C, Yu H, Gong F, Wu H. Induction motor adaptive backstepping control and efficiency optimization based on load observer. Energies. 2020 Jul 19;13(14). https://doi.org/10.3390/en13143712
19. Zhu Y, Lee KY, Wang Y. Adaptive elitist genetic algorithm with improved neighbor routing initialization for electric vehicle routing problems. IEEE Access. 2021 Jan 21;9:16661-71. https://doi.org/10.1109/ACCESS.2021.3053285
20. Hai N, Wang S, Huang Q, Xie Y, Fernandez C. Improved K-means clustering-genetic backpropagation modeling for online state-of-charge estimation of lithium-ion batteries adaptive to low-temperature conditions. Journal of Energy Storage. 2024 Oct 10. https://doi.org/10.1016/j.est.2024.113399
21. Sharma U, Singh B. Design and development of energy efficient single phase induction motor for ceiling fan using Taguchi's orthogonal arrays. IEEE Transactions on Industry Applications. 2021 Apr 8;57(4):3562-72. https://doi.org/10.1109/TIA.2021.3072020
22. Mei J, Zuo Y, Lee CH, Kirtley JL. Modeling and optimizing method for axial flux induction motor of electric vehicles. IEEE Transactions on Vehicular Technology. 2020 Oct 14;69(11):12822-31. https://doi.org/10.1109/TVT.2020.3030280
23. Wang H, Chau KT, Lee CH, Cao L, Lam WH. Design, analysis, and implementation of wireless shaded-pole induction motors. IEEE Transactions on Industrial Electronics. 2020 Jul 10;68(8):6493-503. https://doi.org/10.1109/TIE.2020.3007116
24. Hesari A, Darabi A, Pourmirzaei Deylami F. Dual Independent Rotor Axial Flux Induction Motor for Electric Vehicle Applications. IET Electrical Systems in Transportation. 2024;2024(1). https://doi.org/10.1049/2024/5594289
25. Dianati B, Kahourzade S, Mahmoudi A. Optimization of axial-flux induction motors for the application of electric vehicles considering driving cycles. IEEE Transactions on Energy Conversion. 2020 Feb 27;35(3):1522-33. https://doi.org/10.1109/TEC.2020.2976625